

# Combustion Dynamics at the Top Dead Center Position of a Spark Ignition Engine

## Lucky Anetor

Professor  
Nigerian Defence Academy  
Department of Mechanical Engineering  
Kaduna,  
Nigeria

## Edward E. Osakue

Associate Professor  
Texas Southern University  
Department of Industrial Technologies  
Houston, Texas,  
USA

## Christopher Odetunde

Professor  
Kwara State University  
College of Engineering and Technology  
Malete, Kwara State,  
Nigeria

*A zero-dimensional spark ignition engine model was used to conduct a systematic study of combustion dynamics at the top dead center (TDC) position of a 5.734 liter, V8 spark-ignition engine. The model captures all the experimentally observed essential features concerning combustion at the TDC. The combustion dynamics at compression ratios,  $r_c = 9.5, 10.5, 11.5$  and  $15.5$  and fuel-air equivalence ratio,  $\phi = 1.0$  were investigated with the numerical model. The results show that for  $r_c = 15.5$ , the fuel-oxidizer charge was consumed almost instantaneously. Furthermore, the data shows that it took about 153.0, 52.6, 21.0 and 1.43 ms at compression ratios,  $r_c$  of 9.5, 10.5, 11.5 and 15.5 respectively for the in-cylinder combustion dynamics to reach a value  $T^* = 1.0$ . In the last 0.01 ms, for all compression ratios, the rate of change of pressure,  $dp/dt$  lies in the range  $10^8 < dp/dt < 10^{14}$  Pa/s while the corresponding temperature varies from  $2230 \leq T \leq 2700$  K. The study also shows that as the compression ratio increases both the adiabatic flame temperature and heat of combustion at the top dead center increases monotonically as well.*

**Keywords:** Fuel-air equivalence ratio; Adiabatic flame temperature; Spark ignition engine, Engine knock, Activation energy

## 1. INTRODUCTION

The greatest source of environmental air pollution in urban areas of the world is the automobiles powered by internal combustion engines (ICEs). The pollutants are formed from non-ideal combustion processes which are prevalent in internal combustion engines and their formation depend on both the engine operating parameters (for example, engine temperature, speed, load, fuel-air equivalence ratio, ignition delay, spark timing, exhaust gas recirculation, etc.) as well as the type of fuel. Internal combustion engine emissions consist of volatile organic compounds (VOCs), carbon monoxide (CO) nitric oxide (NO) and nitrous oxide (NO<sub>2</sub>) which are collectively referred to as oxides of nitrogen (NO<sub>x</sub>), particulate matter (PM), carbon dioxide (CO<sub>2</sub>) and water vapor (H<sub>2</sub>O). Volatile organic compounds (VOCs) and (NO<sub>x</sub>) form photochemical smog in the atmosphere, and (CO) and (PM) have been identified as having adverse health impact on humans.

The impacts of fossil fuel combustion in spark ignition engines permeate many areas of our lives, in particular as it relates to economical, sustainability, global climate change and the utilization of energy. In view of the foregoing challenges, research efforts have

focused on designing cost effective, safe, efficient and non-polluting combustion devices for a variety of fossil fuels in such a manner that is economical, protects the environment and support sustainable standard of living.

In order to improve the design of engine combustion systems a thorough understanding of combustion at a fundamental and engineering perspective is required. In-depth understanding of engine combustion is a formidable undertaking that requires a comprehensive knowledge of chemistry, thermodynamics, heat transfer, fluid dynamics and advanced mathematics. For instance, a complete understanding of the most elementary turbulent flame requires detailed knowledge of turbulent reacting flow, a phenomenon which is highly intractable and is presently an area of intensive research. Since it is impracticable to wait until such a time that sufficient knowledge of combustion dynamics is attained, engineers responsible for designing combustion devices have resorted to using a combination of science, experimentation, numerical simulation and experience to look for practicable solutions.

Since the emissions resulting from burning fossil fuels is a major contributor to the formation of photochemical smog and ozone (O<sub>3</sub>) depletion in the stratosphere, its minimization has become a top priority for various national environmental protection agencies.

Presently, a lot of technically feasible strategies could be used to reduce environmental pollution caused by internal combustion engines to acceptable levels. However, these approaches entail some compromise in either performance, reliability or cost.

Received: February 2017, Accepted: May 2017

Correspondence to: Professor Lucky Anetor  
Department of Mechanical Engineering,  
Nigerian Defence Academy, Kaduna, Nigeria  
E-mail: lanetor@uh.edu, anetor55@yahoo.com

doi:10.5937/fmet1704548A

© Faculty of Mechanical Engineering, Belgrade. All rights reserved

FME Transactions (2017) 45, 548-558 548

Therefore, the issue at stake is not really about finding a solution but to look for an optimum combination of solutions. The first step towards achieving this is to have a fundamental understanding of engine combustion processes and the mechanisms by which pollutants are formed. In view of this, the focus of the present study is restricted to spark ignition engines with emphasis placed on combustion dynamics instead of overall engine performance or mechanical design of the automobile.

In other to understand the combustion processes taking place in internal combustion engines, constant- and variable-volume thermochemical reactors/bombs, steady-flow reactors, and rapid compression machines have been used to conduct exploratory studies of the combustion characteristics. These devices are designed in such a manner that the combustion processes of the fuel-air mixtures can be studied under several controlled internal combustion engine-like operating conditions. In the present study the constant- volume thermochemical bomb method was used to simulate the product composition. This study mimics the combustion processes taking place at the top dead center (TDC) position of a spark ignition engine.

## 2. LITERATURE REVIEW

The prevailing pressure on automotive engine manufacturers to increase internal combustion engine's fuel efficiency while simultaneously achieving improved emission levels has spurred a lot of research activities in this field. The reviews contained in this section describe various constant-volume thermochemical reactor/bomb strategies that are presently being used to study combustion processes in spark ignition engines.

Firmansyah, F., et al. [1] investigated the auto-ignition characteristics of dual fuel mixture, namely, diesel and compressed natural gas (CNG) in a constant volume combustion chamber. The Reactivity controlled compression ignition (RCCI) concept was employed. The diesel/compressed natural gas mixture was varied from 0 – 100% diesel/CNG at equivalent ratio of unity. The pressure-crank angle history and high speed photographs of the images of combusting gases were recorded. The results show that diesel/compressed natural gas mixture has superior combustion characteristics when compared to pure diesel. Other results of the study further show that compressed natural gas delayed the combustion process whilst simultaneously enhancing the uniform distribution of diesel within the combustion chamber. It was noticed that the resultant effect created a multipoint ignition of diesel throughout the combustion chamber with the concomitant generation of rapid heat release rate and higher maximum pressure. Furthermore, the study shows that the production of soot was lower when diesel/compressed natural gas mixture was used compared to the case of burning pure diesel.

Hong Guang Zhang, et al., [2] developed a diagnostic method which was used to interpret the results of some combustion studies. The investigation was carried out in a constant volume reactor with

diesel-like fuels. The main objective of the study was to calculate the instantaneous heat release over time from measurements of the combustion chamber pressure-crank angle history. The raw experimental data was filtered in order to remove the oscillations due to the location of the pressure sensor. A semi-empirical heat transfer model was proposed and its coefficients were obtained by fitting them to the experimental data.

Zhang, J., et al. [3] carried out a study with the aim of investigating the combustion of biodiesel and diesel fuels in a constant volume combustion chamber that is optically accessible. The conditions prevalent in compression ignition engines were simulated. The high pressure and temperature environment in the constant volume combustion chamber was achieved by using a controlled premixed combustion with the required excess oxygen. A common rail and an injector with a 160-degree included angle was used in the study. The fuels used in this work were ultra-low sulfur diesel and biodiesel which was obtained from used cooking oil. High speed photography of the luminosity from the flame was used to study the combustion flame in a time-resolved manner. A combination of high speed and intensified imaging of hydroxyl radical chemiluminescence was employed to identify the reaction zones. The effects of various ambient temperature and oxygen concentration on the combustion of both fuels were studied. The results show that an early injection of fuel, representing the higher temperature, experiences a faster auto-ignition, which resulted in less air entrainment in the early stage of flame development. For the ultra-low sulphur diesel it was observed that it produced a higher level of soot, while the effect is less obvious for biodiesel. It was surmised that the formation of soot may be as a result of fuel jet impingement on the combustion chamber wall for both fuels. It was also observed that the high exhaust gas recirculation (EGR) level which was simulated by using 9% oxygen concentration decreases the intensity of the luminosity of the flame, which in turn reduced the flame temperature and soot formation. Similarly, for biodiesel, it was found that the use of high exhaust gas recirculation significantly reduced the soot formation. The authors concluded from the results of their findings that the use of biodiesel as a potential alternative to ultra-low sulphur diesel is quite feasible since it has superior characteristics concerning soot formation when operating at low temperature combustion and elevated EGR levels.

Other research efforts in providing better understanding of combustion efficiency and effective control of combustion emissions can be found in [4 - 12] and the references contained in them.

This paper is organized as follows; the introduction is presented in section 1, followed by the literature review in section 2. Section 3 presents the objectives of the present study, while section 4 describes the models used in this study. Section 5 describes how the model was used to study the combustion process at the top dead center position of a spark ignition engine whose specifications are given in Table 1. The results of the parametric studies are presented in section 6. Finally, some closing remarks and conclusions are presented in section 7.

### 3. OBJECTIVE OF THE PRESENT STUDY

Fossil-fuel derivatives are the main sources of energy which are used in all facets of our daily living. They provide the primary source of energy used in cooking, electricity, manufacturing, transportation, etc. In view of these and the rising environmental pollutions, national security concerns (finite fossil fuel energy sources) and rising cost of fossil fuel, research efforts geared towards investigating combustion efficiency has been reinvigorated. Since the knowledge of product composition and temperature are important because they do affect downstream processes, or simply for environmental considerations that require that pollutant ( $NO_x$ ,  $SO_2$ ,  $CO$ ,  $CO_2$ ,  $O_3$ , etc) concentrations are within permissible limits, hence the need to have a thorough understanding of the combustion processes. As a result of these, the objective of this study is to use a constant volume thermochemical device and various compression ratios,  $r_c = 0.5, 10.5, 11.5$  and  $15.5$  and fuel-air equivalent ratio of unity, that is,  $\phi = 1.0$  to investigate the variation of mass fraction of products of combustion, temperature, pressure and the rate of change of pressure ( $dp/dt$ ) within the combustion chamber of a spark ignition engine. The ultimate goal of this work is to gain a better fundamental understanding of combustion characteristics in internal combustion engines (ICEs) in order to be able to optimize the design of future engines.

### 4. THE ENGINE CYCLE SIMULATION MODEL

In an internal combustion engine the bulk of the combustion reactions take place when both the inlet and exhaust valves are closed. Since there is no inflow and the little outflow through the clearances are negligible and have been ignored, we can model this situation as a constant-mass combustion reactor/bomb with temporal variation of mixture properties. The equations describing the combustion processes can therefore be reduced to their zero-dimensional, unsteady models. It is worth mentioning that the volume of a constant-mass combustion reactor/bomb may or may not have temporal variation.

As stated above, the objective of the present study is to model constant-mass constant-volume combustion reactor, as for example, the combustion processes at the top dead center position of a spark ignition engine (Otto cycle) by simplifying the unsteady, three-dimensional equations which are given below.

This will facilitate the computation of the time history of the reacting mixture from its initial reactant state to its final product state. In general, the product state may or may not be in equilibrium. The main utility of these simplified models are to provide a means of studying the fundamental physics behind the combustion processes in these devices. The results obtained from these models cannot be depended upon solely for practical designs; however, they do provide guidance on the main dynamics inherent in the constant-mass constant-volume combustion reactor/bomb.

### 4.1 CONSERVATION OF MASS EQUATION

The law of conservation of mass for bulk fluid mixtures is given by:

$$\frac{\partial(\rho_m)}{\partial t} + \frac{\partial(\rho_m u_j)}{\partial x_j} = 0 \quad (1)$$

where  $\rho_m$  is the mixture density,  $u_j$  is the fluid velocity with  $j = 1, 2, 3, x_j$  is the coordinate in three mutually perpendicular directions and  $t$  is the time variable.

### 4.2 CONSERVATION OF MASS OF THE SPECIES

The equation of mass transfer of the species can be written as:

$$\frac{\partial(\rho_m \omega_k)}{\partial t} + \frac{\partial(\rho_m u_j \omega_k)}{\partial x_j} = \frac{\partial}{\partial x_j} \left( \rho_m D \frac{\partial \omega_k}{\partial x_j} \right) + R_k \quad (2)$$

where  $k$  is the number of species,  $\omega$  is the mass fraction,  $D$  is the mass diffusivity and  $R_k$  is the volumetric generation rate from chemical reaction.

When Equation (2) is summed over all species  $k$  of the mixture; Equation (1) is obtained. This can be explained as follows; from Dalton's law,  $\rho_m = \sum_k \rho_k$ , since  $\rho_k = \rho_m \omega_k$  and  $\sum_k \omega_k = 1$ . Moreover,  $\sum_k N_{i,k} = \rho_m u_i$ . Therefore, on summing over all species  $k$ , Equation (2) reduces to:

$$\frac{\partial \rho_m}{\partial t} + \frac{\partial(\rho_m u_j)}{\partial x_j} = \sum_k R_k \quad (3)$$

On comparing equation (3) with equation (1), equation (3) becomes exactly equal to equation (1) when  $\sum_k R_k = 0$  the physical interpretation of this is that when some species are generated by for example a chemical reaction, some others are consumed by combustion in the case of an ice. This implies that there is no net mass generation in the bulk fluid.

### 4.3 CONSERVATION OF CHEMICAL ELEMENTS

It can be shown [13] that the mass fraction  $\eta_\alpha$  of chemical element  $\alpha$  in the mixture of a chemical reaction mechanism containing  $k$  species, is given by:

$$\eta_\alpha = \sum_k \eta_{\alpha,k} \omega_k \quad (4)$$

where  $\eta_{\alpha,k}$  is the mass fraction of element  $\alpha$  in species  $k$ . In a manner analogous to species convection, diffusion, generation and consumption/destruction so also are the elements in a chemical reaction. However, the chemical elements can neither be destroyed nor created/generated in view of the principle of conservation of element (law of definite proportions). Therefore, the transport equation for any chemical element  $\alpha$  will have no source term. Hence, the conservation of element equation is given by:

$$\frac{\partial(\rho_m \eta_\alpha)}{\partial t} + \frac{\partial(\rho_m u_j \eta_\alpha)}{\partial x_j} = \frac{\partial}{\partial x_j} \left( \rho_m D \frac{\partial \eta_\alpha}{\partial x_j} \right) \quad (5)$$

Notice that the diffusion coefficient  $D$  for the elements is assumed to be equal to those of the species [14].

### 4.3 ENERGY EQUATION

In combustion calculations, it is more convenient to use the enthalpy or the temperature forms of the energy equation. It can be shown that the energy equations in enthalpy and temperature forms are given by [13]:

$$\rho_m \frac{Dh_m}{Dt} = \frac{\partial}{\partial x_j} \left( k_{eff} \frac{\partial T}{\partial x_j} \right) - \frac{\partial \left( \sum m_{j,k}^n h_k \right)}{\partial x_j} \quad (6)$$

$$+ \mu \Phi_v + \frac{Dp}{Dt} + \dot{Q}_{rad} + \dot{Q}_{others}$$

and the energy equation in terms of temperature is:

$$\rho_m c_{p_m} \frac{DT}{Dt} = \frac{\partial}{\partial x_j} \left( k_{eff} \frac{\partial T}{\partial x_j} \right) + \mu \Phi_v + \frac{Dp}{Dt} \quad (7)$$

$$+ \dot{Q}_{rad} + \dot{Q}_{others} - \sum_k \left( h_{f,k}^0 + \Delta h_{s,k} \right) R_k$$

where  $T$  is the temperature,  $c_{p_m}$  is the specific heat at constant pressure of the mixture,  $h_m$  is the enthalpy of the mixture,  $h_k$  is the enthalpy of species  $k$ ,  $k_{eff} = k_m + k_t$  is the effective conductivity,  $k_m$  is the conductivity of the mixture and  $k_t$  is the turbulent conductivity,  $\dot{Q}_{rad}$  and  $\dot{Q}_{others}$  are the volumetric generation/dissipation from radiation and other sources respectively. The viscous dissipation function is  $\Phi_v$  and  $\mu$  is the molecular viscosity.

The following important remarks concerning the energy equation in temperature form are worth mentioning:

1.  $-\sum_k h_{f,k}^0 R_k = \dot{Q}_{chem}$  is the net volumetric rate of heat generation as a result of chemical reaction. For a simple chemical reaction (SCR),  $\dot{Q}_{chem} = R_{fu} \Delta H_c$  where  $H_c$  is the enthalpy of formation.
2. If we assume that the specific heats of all species are equal, that is,  $C_{p_j} = C_{p_m} = C_p$  then  $\sum_k \Delta h_{s,k} R_k = 0$ . The last term in Equation (7) is also zero because  $\sum_k D \partial \omega_k / \partial x_j = 0$ .
3. The viscous dissipation terms  $\mu \Phi_v$  are significant only in high Mach number flows. Similarly, the  $Dp/Dt$  term is important in compressible flows particularly when shock waves are present.

### 5. MODELLING COMBUSTION AT TOP DEAD CENTRE IN ICE

In internal combustion engines, the combustion taking place at the top dead center position can be modeled as a constant-mass constant-volume process whereas when the engine is in the normal operational mode, the combustion dynamics can be treated as a constant mass variable volume process.

In the present paper parametric studies of the effects of fuel-air equivalent ratio on pressure and temperature history as well as on the products of combustion was undertaken for both types of combustion processes. In order to accomplish this, Equations (1) to (7) were reduced to the following appropriate forms:

#### 5.1 MODELING CONSTANT VOLUME REACTOR

In constant-volume constant-mass reactor, there are neither inflows nor outflows. Therefore, if the volume of the reactor,  $V$  is constant, then, the equations of bulk mass, mass transfer and energy reduces to:

$$\frac{d(\rho_m V)}{dt} = 0 \quad (8)$$

$$\frac{d(\rho_j V)}{dt} = \frac{d(\rho_m V \omega_j)}{dt} = R_j V \quad (9)$$

and

$$\frac{d(\rho_m V e_m)}{dt} = \dot{Q}_{rad} - \dot{W}_{exp} + q_w A_w \quad (10)$$

where  $q_w A_w$  is the reactor wall heat transfer. The wall heat transfer specified here is in generalized form. In the present study the wall heat transfer is assumed to be adiabatic, hence,  $q_w A_w = 0$ . However, when all the processes of an internal combustion cycle is considered, the heat transfer model described in [17] is normally used.  $\dot{W}_{exp} = p \times dV / dt$  is the expansion work transfer,  $p$  is the pressure and  $e_m$  is the specific energy of the mixture, and it is given by:  $e_m = h_m - p/\rho_m$ .

For a constant-volume constant-mass system,  $V$  is constant hence  $\dot{W}_{exp} = p \times dV / dt = 0$ .

The derivation of the models presented so far assume that temperature and mass fractions are uniform all over the combustion chamber volume at all times. That is, the state of the products of combustion is assumed to be isotropic; this type of representation is referred to as thermodynamic model. However, in practical combustion devices, the ignition process creates substantial spatial and temporal variations of temperature and mass fractions as the flame front propagates through the unburned mixture. Sometimes, the air-fuel mixture resulting from pressure and temperature rise during the compression stroke, may auto-ignite, thereby leading to engine knock, which most often causes substantial damage to the piston-crank assembly. It is for this reason that an accurate model of the rate of pressure rise is highly important.

#### 5.2 SIMULATION OF A CONSTANT-MASS CONSTANT-VOLUME REACTOR/BOMB

As stated above, in an internal combustion engine, ignition is initiated a few crank angle degrees before top dead center (BTC) and a greater portion of the fuel-air mixture is burnt at constant volume while the

combustion of the remaining unburnt charge propagates further into parts of the expansion stroke. Therefore, strictly speaking, in a constant-mass reactor, combustion can either be approximated as a constant-volume or a variable-volume process. In the constant-mass variable-volume scenario, the combustion chamber volume,  $V$  will vary with time and it can be determined from the speed,  $N$  of the engine and the dimensions of the connecting rod and crank which are connected to the piston. The constant-mass constant-volume, that is, combustion at the top dead center (TDC) position is studied in the present work by using appropriately transformed versions of Equations (1) to (10).

The scenario used to illustrate the constant-mass constant-volume reactor/bomb combustion process is described below.

A mixture of  $n$ -octane, ( $C_8H_{18}$ ) and moist air ( $\phi = 1.0$ ,  $x_{H_2O} = 0.02$ ) is drawn into an engine at a temperature,  $T = 300K$  and pressure,  $p = 1.01325 \text{ bar}$ . It is required to investigate the time histories of  $T$ ,  $p$ ,  $dp/dt$  and the mass fractions  $\omega_{C_8H_{18}}$ ,  $\omega_{O_2}$ ,  $\omega_{CO_2}$  and  $\omega_{H_2O}$  until extinction (that is, until the fuel is totally consumed) at compression ratios,  $r_c = 9.5, 10.5, 11.5$  and  $15.5$  and fuel-air equivalence ratio,  $\phi = 1.0$ . In the present study it is assumed that compression is isentropic, that is,  $\gamma = 1.4$ . It is desired to investigate the heat of combustion,  $\Delta H_c(TDC)$  and the adiabatic flame temperature,  $T_{ad}$ . It is assumed that  $c_{p_j} = c_{p_m} = 1200 \text{ J/Kg}\cdot K$  and mixture molecular mass,  $M_m = 29$ . The objective is to simulate the combustion processes of  $n$ -octane, ( $C_8H_{18}$ )-air mixture in a constant-volume constant-mass reactor at the TDC position. A one-step thermochemical reaction model at the top dead center position is assumed in the present study.

In order to simulate the conditions described in sections 5.1 and 5.2, the following assumptions regarding the thermodynamics and the chemical kinetics were made.

1. One-step global kinetics and the following engineering approximation for global reaction was made [18]:



$$\frac{d[C_xH_y]}{dt} = -A_F \exp\left(-\frac{E_a}{R_u T}\right) [C_xH_y]^m [O_2]^n \quad (12)$$

where  $[*] \triangleq \text{kmol} / \text{m}^3 \cdot \text{s}$ .

For  $n$ -octane:  $A_F = 4.049 \times 10^{10}$ ,  $E_a/R_u = 20131$ ,  $m = 0.25$ ,  $n = 1.5$

$k_G$  is the global rate coefficient,  $E_a$  is the activation energy,  $R_u$  is the universal gas constant,  $T$  is temperature in Kelvin,  $m$  and  $n$  are exponential parameters,  $x$  and  $y$  are the number of carbon and hydrogen atoms respectively in the fuel.

2. The specific heats at constant pressure of the fuel, air and products are constant and equal,

that is,  $c_{pF} = c_{pOX} = c_{pP} = 1200 \text{ J/Kg}\cdot K$  and the molecular weight of the mixture,  $M_m = 29$ .

3. In the present study the stoichiometric air-fuel ratio is 15.05 and combustion is constrained to stoichiometric or lean burn conditions, that is,  $\phi \leq 1.0$ .

The value of the parameters,  $A$ ,  $E_a/R_u$ ,  $m$  and  $n$  were chosen in such a manner that they give the best agreement when experimental and predicted flame speeds and flammability limits are compared [18].

### 5.3 NUMERICAL SOLUTION

The numerical solution which was used to solve the situation described in sections 5.1 and 5.2 is as follows:

Since  $V$  is constant, Equation (8), reduces to  $d\rho_m/dt = 0$ , or  $\rho_m = \text{constant}$ , although  $p$  and  $T$  varies with time.

Therefore, Equations (9) and (10) transform to:

$$\frac{d(\omega_{C_8H_{18}})}{dt} = -\frac{|R_{C_8H_{18}}|}{\rho_m} \quad (13)$$

$$\frac{d(\omega_{O_2})}{dt} = -\frac{|R_{O_2}|}{\rho_m} \quad (14)$$

$$\frac{d(\omega_{CO_2})}{dt} = -\frac{|R_{CO_2}|}{\rho_m} \quad (15)$$

$$\frac{d(\omega_{H_2O})}{dt} = -\frac{|R_{H_2O}|}{\rho_m} \quad (16)$$

$$\frac{d(\omega_{N_2})}{dt} = 0 \quad (17)$$

$$\rho_m \frac{d\varepsilon}{dt} = 0 \Rightarrow \frac{d}{dt} \left( h_m - \frac{p}{\rho_m} \right) =$$

$$\rho_m \frac{d}{dt} (c_{p_m} T + \Delta H_c \omega_{C_8H_{18}} - R_{mix} T) = 0, \text{ or} \quad (18)$$

$$\Rightarrow \rho_m \frac{d}{dt} (c_{v_m} T) + \left[ \rho_m \frac{d(\omega_{C_8H_{18}})}{dt} \right] \Delta H_c = 0$$

where  $c_{v_m} = c_{p_m} - R_{mix}$ .

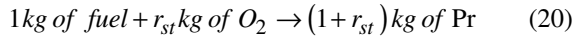
From the foregoing, the net consumption rate of  $C_8H_{18}$  is given by:

$$|R_{C_8H_{18}}| = MW_{C_8H_{18}} \times \left| -A_F \exp\left(-\frac{E_a}{R_u T}\right) [C_8H_{18}]^{0.25} [O_2]^{1.5} \right|$$

Therefore:

$$|R_{C_8H_{18}}| = \left| -A_F \exp(-E_a/R_u T) \cdot \rho_m^{1.75} \frac{M^{.75} C_8H_{18}}{M^{1.5} O_2} \omega^{.25} C_8H_{18} \omega^{1.5} O_2 \right| \quad (19)$$

Since a single-step global mechanism which also referred to as simple chemical reaction is assumed in the present study, then:



where Pr is the products of combustion and  $r_{st}$  is the stoichiometric ratio and is defined as:

$$r_{st} = \frac{MW_{O_2}}{MW_F}, a_{stoic} = \frac{MW_{O_2}}{MW_F} \left( m + \frac{n}{4} \right)$$

Therefore:

$$R_{O_2} = r_{st} R_F \text{ and } R_p = -(1 + r_{st}) R_F \quad (21)$$

From the stoichiometric combustion of  $n$ -octane, ( $C_8H_{18}$ ):

$$R_{O_2} = r_{st} R_{C_8H_{18}} \text{ and } R_{CO_2} = R_{H_2O} = -(1 + r_{st}) R_{C_8H_{18}}$$

On combining Equations (13) to (18), we get:

$$\left[ \omega_{C_8H_{18}} - \frac{\omega_{O_2}}{r_{st}} \right]_t = \left[ \omega_{C_8H_{18}} - \frac{\omega_{O_2}}{r_{st}} \right]_i \quad (22)$$

$$\left[ \omega_{C_8H_{18}} + \frac{\omega_{CO_2}}{(1 + r_{st})} \right]_t = \left[ \omega_{C_8H_{18}} + \frac{\omega_{CO_2}}{(1 + r_{st})} \right]_i \quad (23)$$

$$\left[ \omega_{C_8H_{18}} + \frac{\omega_{H_2O}}{(1 + r_{st})} \right]_t = \left[ \omega_{C_8H_{18}} + \frac{\omega_{H_2O}}{(1 + r_{st})} \right]_i \quad (24)$$

and

$$\left[ \omega_{C_8H_{18}} + \frac{c_{vm} T}{\Delta H_c} \right]_t = \left[ \omega_{C_8H_{18}} + \frac{c_{vm} T}{\Delta H_c} \right]_i \quad (25)$$

From Equations (22) to (25),  $\omega_{C_8H_{18}}$ ,  $\omega_{O_2}$ ,  $\omega_{CO_2}$  and  $\omega_{H_2O}$  can be expressed as functions of temperature  $T$ , when their initial reactant values are known. The initial values are solved for as follows:

The initial reactants,  $R_{react}$  are:

$$R_{react} = C_8H_{18} + \frac{12.5}{\phi} (O_2 + 3.76N_2) + n_{H_2O} H_2O$$

where  $n_{H_2O}$  is the initial number of moles of water vapor,  $H_2O$  The mole fraction,  $x_{H_2O}$  of water vapor is given by:

$$\frac{n_{H_2O}}{1 + 12.5 \times 4.76 / \phi + n_{H_2O}} = x_{H_2O} = 0.02 \quad (26)$$

$$\text{Hence: } n_{H_2O} = 1.234$$

Therefore, the initial reactant mass,  $M_{R_i} = 114 + 12.5(32 + 3.76 \times 28) + 1.2347 \times 18 = 1852.2246$

Hence,  $\omega_{C_8H_{18}} = 114/1852.2246 = 0.06155$  similar-ly,  $\omega_{O_2_i} = 0.21596$ ,  $\omega_{N_2_i} = 0.71050$  and  $\omega_{H_2O_i} = 0.012$  and  $\omega_{CO_2_i} = 0$ .

With the initial values/conditions known, Equation (19) becomes:

$$\begin{aligned} \frac{d}{dt} (c_{vm} T) &= RHS = \frac{\Delta H_c}{\rho_m} \times |R_{C_8H_{18}}| \\ &= \left| -A_F \exp \left( -\frac{E_a}{R_u T} \right) \rho_m^{1.75} \cdot \frac{MW_{C_8H_{18}}^{0.75}}{MW_{O_2}^{1.5}} \cdot \omega_{C_8H_{18}}^{0.25} \cdot \omega_{O_2}^{1.5} \right| \end{aligned} \quad (27)$$

where:

$$\omega_{C_8H_{18}} = \omega_{C_8H_{18_i}} - c_{vm} (T - T_i)$$

$$\omega_{O_2} = \omega_{O_2} + r_{st} (\omega_{C_8H_{18}} - \omega_{C_8H_{18_i}}) \Rightarrow \omega_{O_2}$$

$$= \omega_{O_2_i} - r_{st} \frac{c_{vm}}{\Delta H_c} (T - T_i)$$

$$\omega_{CO_2} = \omega_{CO_2_i} - (1 + r_{st}) (\omega_{C_8H_{18}} - \omega_{C_8H_{18_i}}) \Rightarrow$$

$$\omega_{CO_2} = (1 + r_{st}) \frac{c_{vm}}{\Delta H_c} (T - T_i)$$

$$\omega_{H_2O} = \omega_{H_2O_i} - (1 + r_{st}) (\omega_{C_8H_{18}} - \omega_{C_8H_{18_i}}) \Rightarrow$$

$$\omega_{H_2O} = \omega_{H_2O_i} + (1 + r_{st}) \frac{c_{vm}}{\Delta H_c} (T - T_i)$$

In order to complete the modeling of the right hand side (RHS) of Equation (27), we have to model the values of  $\rho_m$ ,  $c_{vm}$  and  $\Delta H_c$  as well. These quantities are modeled as:

$\Delta H_c = (H_{reaction} - H_{product})$ , similarly, the adiabatic flame temperature,  $T_{ad}$  is computed for the combustion temperature  $T$  and equivalent ratio,  $\phi$ . While the extinction temperature,  $T_{ext}$  corresponds to the value of  $\omega_{C_8H_{18}}$  such that  $\omega_{C_8H_{18}} = 0$ .

$c_{vm} = \sum_j \omega_j c_{v_j} = \sum_j (c_{p_j} - R_u / M_j)$ , where  $c_{p_j}$  is evaluated as a function of temperature,  $T$  at each instant of time during the computation of Equation (27). Finally,  $\rho_m = p M_m / (R_u T)$ , where  $M_m = (\sum_j \omega_j M_j)^{-1}$ . Since the volume is constant,

$$\frac{p}{R_m T} = \left( \frac{p}{R_m T} \right)_i \quad (28)$$

From Equation (28), the instantaneous values of  $p$  can be computed. Furthermore, Equation (27) can now be expressed as:

$$\left( c_{vm} T \right)_{t+\Delta t} = \left( c_{vm} T \right)_t + RHS (T_t) \cdot \Delta t \quad (29)$$

In the present study the Euler's integration computational method was used to solve Equation (29) which models the constant-mass constant-volume combustion dynamics, at every instant of time,  $t$ . The time-step,  $\Delta t$ , which was used in the present study, is 1.0 ms. However,  $\Delta t$  was gradually reduced as  $T^* = (T - T_i) / (T_{ad} - T_i) \rightarrow 1.0$ , in order to preserve accuracy. Simulations are terminated when  $\omega_{C_8H_{18}} \leq 0$  and the

flame is extinguished, that is, the fuel ( $C_8H_{18}$ ) has been totally consumed.

## 5.4 INITIAL CONDITIONS

In order to complete the necessary input information, the relevant initial conditions for the first order differential equation which describes the interactions between temperature, pressure and mass fractions are specified thus:

- Initial conditions - temperature:  
 $T = T_i = T_{amb} \cdot (r_c)^{0.4} = 0$
- Initial conditions - pressure:  
 $p = p_i = p_{amb} \cdot (r_c)^{1.4}$  at  $t = 0$
- Initial conditions - mass fraction of species: at  $t = 0$ ,  $\{\omega_{C_8H_{18}}, \omega_{O_2}, \omega_{CO_2}, \omega_{H_2O}\}_i$  refer to Eq. (26).

## 5.5 CONVERGENCE CRITERIA

For the zero dimensional model used in the present study, convergence was obtained after 17 iterations at each time step. The local truncation, discretization and global errors are on the order of  $O(\Delta t^2)$ ,  $O(\Delta t)$  and  $O(\Delta t)$  respectively for the Euler integration scheme. In view of these, convergence criterion was set to a tolerance value of  $10^{-6}$ . Therefore, complete calculations are repeated until the final values converge to within the specified tolerance with the initial values.

## 6. RESULTS

The results presented in this study were obtained from a 5.734 liter, V8 engine. Table 1 below lists the engine specifications, operating conditions and fuel input parameters.

The data presented shows the temporal variation of several important parameters which are useful to internal combustion engine performance at various compression ratios,  $r_c$ . The quantities are combustion chamber pressure, rate of change of combustion chamber pressure with time, combustion chamber temperature, adiabatic flame temperature, heat of combustion at TDC and variation of mass fractions of fuel, water vapor, carbon dioxide and oxidizer. The operating conditions investigated are clearly annotated in Figures 1 - 10. Comprehensive discussions of the effects of engine compression ratio are presented in the paragraphs that follow.

Figures 1 and 2 show the variation of combustion cylinder pressure and the rate of change of combustion cylinder pressure versus time. The figures show that as compression ratio increases the pressures and the rate of change of pressure increases as well. However, it can be seen from Figures 1 and 2 that at compression ratios in the range  $9.5 \leq r_c \leq 11.5$ , the rise in both pressure and rate of change of pressure are quite smooth and somewhat gradual for most of portions of the combustion processes, thereafter, a rapid consumption of the remaining charge ensues. The gradual combustion processes that were witnessed for compression ratios in the range  $9.5 \leq r_c \leq 11.5$  was completely absent for compression ratio,  $r_c = 15.5$ , Figures 1 and 2 show that for  $r_c = 15.5$ , the fuel-

oxidizer charge was consumed almost instantaneously as can be seen from these characteristics which are almost vertical. This shows a high likelihood of engine knock, therefore, operating a spark ignition engine with compression ratio,  $r_c \geq 15$  should be avoided unless of course some specially treated fuels are used.

The variation of in-cylinder temperature with time and the graph of adiabatic flame versus compression ratio,  $r_c$  are shown in Figures 3 and 4 respectively. The shapes of the pressure and rate of change of pressure with time shown in Figures 1 and 2 are positively correlated with the temperature characteristics shown in Figure 3 as expected. Figure 4 shows that as compression ratio increases the adiabatic flame temperature increases as well.

However, the temperature gradient is steeper for compression ratios in the range,  $9.5 \leq r_c \leq 11.5$  than compression ratios,  $11.5 \leq r_c \leq 15.5$ . The results show that it took about 153.0, 52.6, 21.0 and 1.43 ms at compression ratios,  $r_c$  of 9.5, 10.5, 11.5 and 15.5 respectively for the in-cylinder combustion dynamics to reach  $T^* = 1.0$ . In the last 0.01 ms, for all compression ratios the rate of change of pressure,  $dp/dt$  lies in the range  $10^8 < dp/dt \leq 10^{14}$  Pa/s and the corresponding temperature varies from  $2230 \leq T \leq 2700$  K. The rapid change in temperature and pressure with corresponding high rate of depletion of fuel-oxidizer ( $C_8H_{18} - O_2$ ) mixture characterizes thermochemical explosion, that is, engine knock.

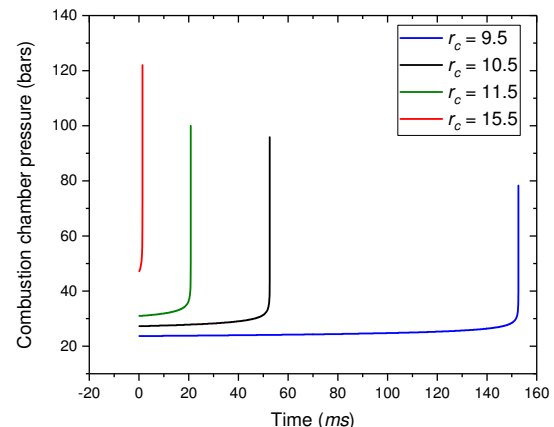


Figure 1. Variation of combustion chamber pressure with time at compression ratios,  $r_c$

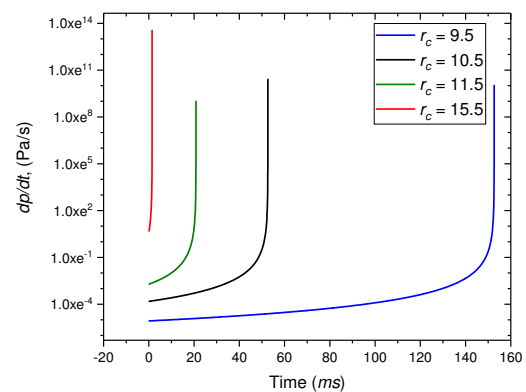


Figure 2. Graph of  $dp/dt$  versus time at compression ratios,  $r_c$

This phenomenon is due to the extremely fast interaction between the energy released and the

corresponding temperature rise from the combustion reaction which in turn feeds back to produce constantly increasing reaction rates because of the dependence of temperature on the reaction rate, that is,  $(-E_a/RT)$ , where  $E_a$  is the activation energy.

Figures 5 and 6 show the variation of heat of combustion at the top dead center position versus compression ratio and adiabatic flame temperature for compression ratios in the range  $9.5 \leq r_c \leq 11.5$  respectively. It can be seen from Figure 5 that as the compression ratio increases the heat of combustion at the top dead center increases monotonically. This can be explained from the characteristics exhibited in Figure 6, namely, as the adiabatic flame temperature increases the heat of combustion at the top dead center position increases sharply as well. This is due to fact that the compression stroke preheats the ( $C_8H_{18} - O_2$ )mixture, thereby increasing the adiabatic flame temperature with the concomitant steep increase in the heat of combustion at the top dead center shown in Figures 5 and 6.

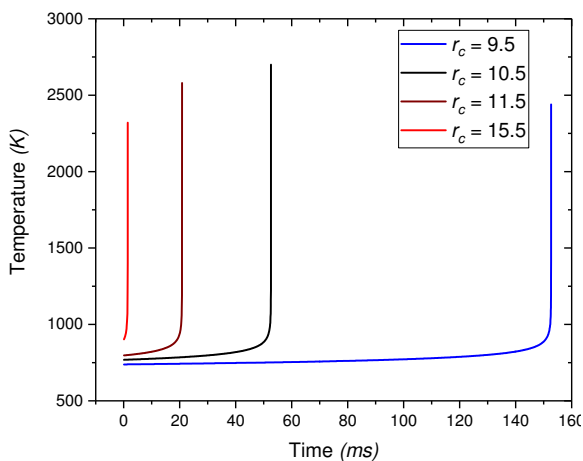


Figure 3. Graph of combustion chamber temperature versus time at compression ratios,  $r_c$

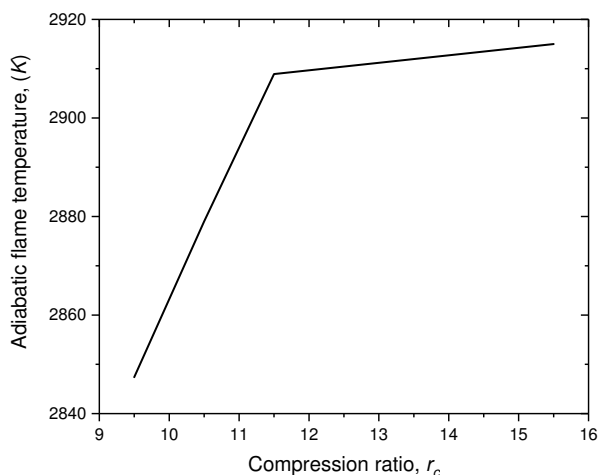


Figure 4. Graph of adiabatic flame temperature versus compression ratio,  $r_c$

Figures 7 and 8 show the mass fractions of fuel and oxidizer versus time at compression ratios,  $9.5 \leq r_c \leq 11.5$  respectively. The graphs also show that the characteristics of the fuel and oxidizer mass fractions are perfectly correlated. From Figures 7 and 8, it can be

seen that the fuel-oxidizer mixture were consumed almost instantly consumed, that is, at a total time of 1.43 ms for compression ratio,  $r_c = 15.5$  whereas the fuel-oxidizer was consumed at a much gradual rate for compression ratios in the range  $9.5 \leq r_c \leq 11.5$ .

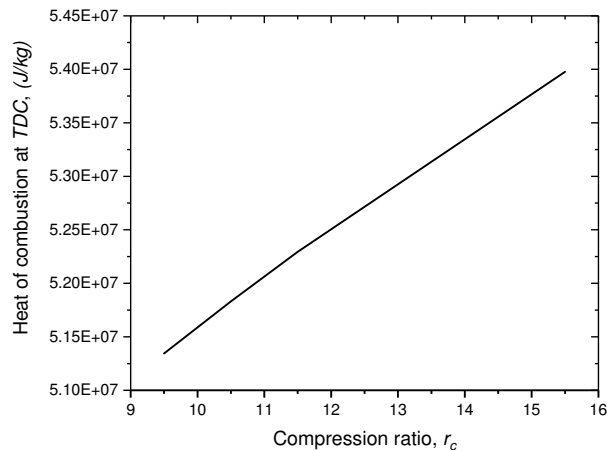


Figure 5. Graph of heat of combustion at TDC versus compression ratio,  $r_c$

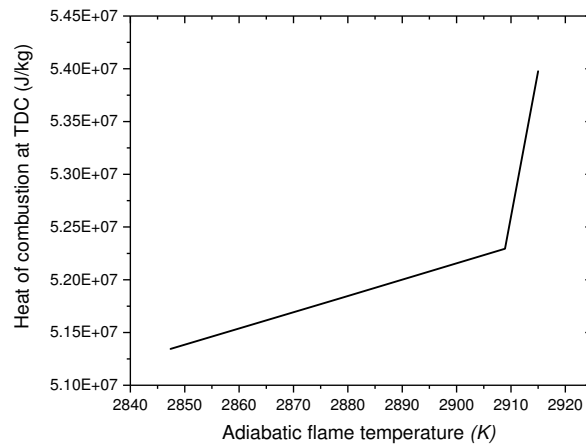


Figure 6. Graph of heat of combustion at TDC versus adiabatic flame temperature  $9.5 \leq r_c \leq 11.5$

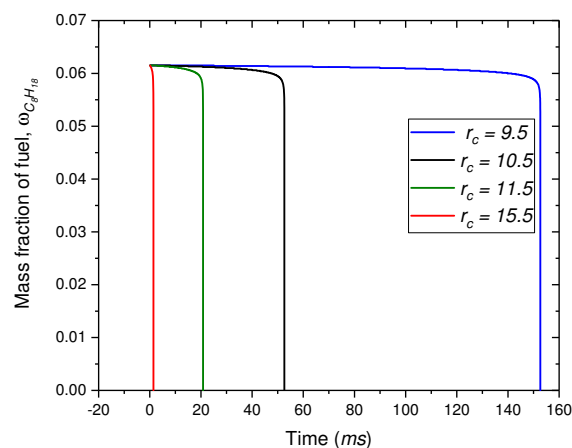


Figure 7. Graph of mass fraction of fuel versus time at compression ratios,  $r_c$

The graphs of mass fractions of carbon dioxide ( $CO_2$ ) and water vapor ( $H_2O$ ) produced versus time at compression ratios  $9.5 \leq r_c \leq 11.5$  are shown in Figures 9 and 10 respectively. The graphs show that the trends are positively correlated to a very high degree. It can

be seen from Figures 9 and 10 that the least amount of carbon dioxide ( $\text{CO}_2$ ) and water vapor ( $\text{H}_2\text{O}$ ) were produced at a compression ratio,  $r_c = 15.5$ . This could be due to that fact that because combustion was so fast with the concomitant high temperature a good fraction of the carbon dioxide ( $\text{CO}_2$ ) and water vapor ( $\text{H}_2\text{O}$ ) may have dissociated to form other species.

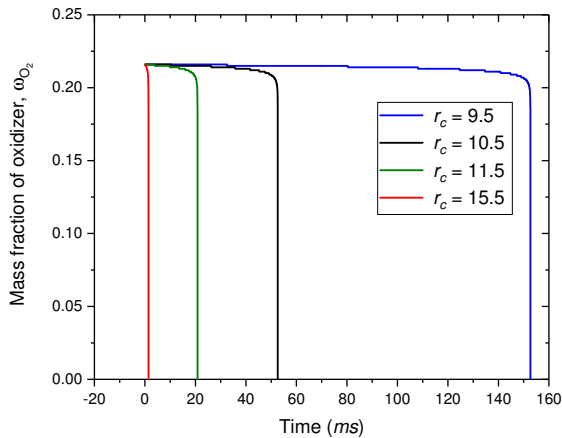


Figure 8. Graph of mass fraction of oxidizer versus time at compression ratios,  $r_c$

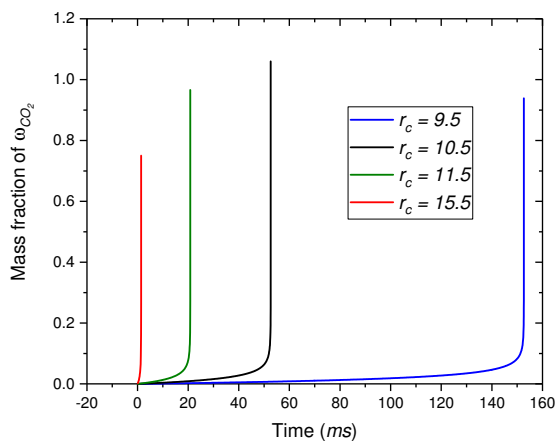


Figure 9. Graph of mass fraction of  $\text{CO}_2$  produced versus time at compression ratios,  $r_c$

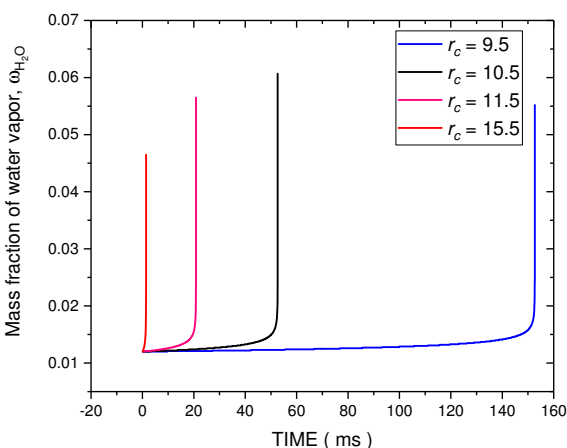


Figure 10. Graph of mass fraction of  $\text{H}_2\text{O}$  vapor produced versus time at compression ratios,  $r_c$

## 7. REMARKS AND CONCLUSION

A zero-dimensional model was used to investigate combustion dynamics of a 5.734 liter, V8 spark-

ignition engine at the top dead center position. Some remarks and conclusion concerning the results from this study are provided in sections 7.1 and 7.2 below.

### 7.1 REMARKS

It is worth mentioning that although the simulated results presented in this study predicts the explosive combustion of the octane ( $\text{C}_8\text{H}_{18}$ ) - oxidizer mixture after an initial period of gradual combustion, as usually observed in practical spark ignition engine combustion and the knocking experienced on a few occasion; single-step kinetic mechanisms do not model the actual characteristics of auto-ignition in fuel-oxidizer mixtures. In reality, the induction or ignition delay period, is governed by formation of intermediate species (radicals), therefore, in order to accurately simulate knock, a more detailed mechanism should be used.

The model presented in this study did not consider the effect of residual combustion products and the compression process was assumed to be isentropic. In view of these, the values produced by the model are more likely to be higher than those observed in practical spark ignition engines. This is due to the fact that in real engines, the combustion chamber wall is cooled by an engine coolant that is at a lower temperature than the combustion gases inside the engine combustion chamber. Since there is heat transfer between the hot combustion gases and the coolant, the compression process would not be truly isentropic; a more accurate model would be a polytropic compression process.

### 7.2 CONCLUSION

As stated above, a zero-dimensional model was used to investigate combustion dynamics of a 5.734 liter, V8 spark-ignition engine at the top dead center position. The code captures all the experimentally observed essential features concerning combustion at the top dead center position. This capability could be viewed as an accomplishment which would be impossible to realize in a reasonable amount of time had experimentation been undertaken. The results are shown in Figures 1 to 10.

In specifics, the conclusions from this study can be summarized as follows:

1. Figures 1 and 2 show that for  $r_c = 15.5$ , the fuel-oxidizer charge was consumed almost instantaneously as can be seen from there characteristics which are almost vertical. This shows a high likelihood of engine knock.
2. The results show that it took about 153.0, 52.6, 21.0 and 1.43 ms at compression ratios,  $r_c$  of 9.5, 10.5, 11.5 and 15.5 respectively for the in-cylinder combustion dynamics to reach a value  $T^* = 1.0$ . In the last 0.01 ms, for all compression ratios the rate of change of pressure,  $dp/dt$  lies in the range  $10^8 < dp/dt \leq 10^{14}$  Pa/s and the corresponding temperature varies from  $2230 \leq T \leq 2700$  K.
3. The results show that as the compression ratio increases the heat of combustion at the top dead center increases monotonically, refer to Figure 5.

4. The least amount of carbon dioxide (CO<sub>2</sub>) and water vapor (H<sub>2</sub>O) were produced at a compression ratio,  $r_c = 15.5$  see Figures 9 and 10.

**Table 1. Engine specifications and operating conditions**

Parameter	Value
Number of cylinders, $n_c$	8
Engine speed, (rpm)	2200
Bore, $d$ (mm)	101.6
Stroke, $L$ (mm)	88.4
Compression ratios, $r_c$	9.5, 10.5, 11.5 and 15.5
Ambient temperature, $T_{amb}$ (K)	300
Ambient pressure, $p_{amb}$ (bar)	1.01325
Cylinder wall temperature, $T_w$ (K)	650
Initial temperatures, $T_i$ (K)	738.26, 768.42, 796.89 and 897.95
Initial pressures, $p_i$ (bar)	23.69, 27.25, 30.95 and 47.01
Fuel, $n$ -octane	C <sub>8</sub> H <sub>18</sub>
Fuel-air equivalence ratio, $\phi$	1.0

#### ACKNOWLEDGMENT

The work reported herein was graciously supported by the Nigerian Defence Academy, Kaduna, Nigeria, Texas Southern University, Houston, Texas, USA and the Kwara State University, Malete, Nigeria.

#### REFERENCES

[1] Firmansyah, F., Aziz, A.R.A. and Heikal, M.R.: The combustion behavior of diesel/CNG mixtures in a constant volume combustion chamber, 3rd International Conference of Mechanical Engineering Research (ICMER 2015), IOP Conf. Series: Materials Science and Engineering 100 (2015) 012032. DOI: 10.1088/1757-899X/100/1/012032, 2015.

[2] Hong Guang Zhang, Xiao Lei Bai, Dong Soo Jeong, Gyu Back Cho, Su Jin Choi, Jin Soo Lee, Science China Technological Sciences, Volume 53, Issue 4, pp 1000–1007, 2010.

[3] Zhang, J. and Fang, T., Spray Combustion of Biodiesel and Diesel in a Constant Volume Combustion Chamber, SAE Technical Paper 2011-01-1380, 2011. doi:10.4271/2011-01-1380.

[4] Luijten, C.C.M., Doosje, E. and de Goey, L.P.H., Accurate analytical models for fractional pressure rise in constant volume combustion, International Journal of Thermal Sciences, Volume 48, Issue 6, Pages 1213-1222, June 2009.

[5] Zhang, J. and Fang, T., Spray Combustion of Biodiesel and Diesel in a Constant Volume Combustion Chamber, SAE Technical Paper 2011-01-1380, 2011, doi:10.4271/2011-01-1380.

[6] Liu, H., et al., Spray and Combustion Characteristics of  $n$ -Butanol in a Constant Volume Combustion Chamber at Different Oxygen Concentrations, SAE Technical Paper 2011-01-1190, 2011, doi:10.4271/2011-01-1190.

[7] Lt. Col. lect. Dr. Ing. Daniel Antonie, Col.(r). Prof. AS. Dr. Ing. Sorin Gheorghian, Col. (r). C.S.II Dr. Ing. Nicolae Mărușțelu, Modeling of Constant

Volume Combustion of Propellants for Artillery Weapons, Military Technical Academy, Bucharest, Roman. <http://www.agir.ro/buletine/1739.pdf>

[8] Bernhard C. Bobusch, Phillip Berndt, Christian O. Paschereit, and Rupert Klein, Shockless Explosion Combustion: An Innovative Way of Efficient Constant Volume Combustion in Gas Turbines, Combustion Science and Technology Vol. 186, Issue 10 - 11, 2014.

[9] Feng Yan and Wanhua Su, Numerical Study on Exergy Losses of  $n$ -Heptane Constant-Volume Combustion by Detailed Chemical Kinetics, Energy Fuels, 2014, 28 (10), pp 6635–6643. DOI: 10.1021/ef5013374

[10] Nathan Ian David Hinton, (2014). Measuring laminar burning velocities using constant volume combustion vessel techniques. D. Phil. University of Oxford. <https://ora.ox.ac.uk:443/objects/uuid:5b641b04-8040-4d49-a7e8-aae0b0ffc8b5>

[11] Travis, Jeffrey Todd, A Computational Investigation of a Constant Volume Combustion Jet Engine, PhD. Thesis, North Carolina State University, 3586223, 184 pages, 2014.

[12] Phan, Anthony, Development of a Rate of Injection Bench and Constant Volume Combustion Chamber for Diesel Spray Diagnostics, Graduate Theses and Dissertations. Paper 10691, Iowa State University, Ames, Iowa, 2009.

[13] Anil W. Date, Analytic Combustion - With Thermodynamics, Chemical Kinetics, and Mass Transfer, 32 Avenue of the Americas, New York, NY 10013-2473, USA. ISBN 978-1-107-00286-9, 2011.

[14] Kays, W. M. and Crawford M. E., Convective Heat and Mass Transfer. 3rd ed., McGraw-Hill, New York, 1993.

[15] Colin R. Ferguson and Allan T. Kirkpatrick, Internal Combustion Engines, Applied Thermosciences, Third Edition, Wiley Publishers, 2015.

[16] Borman G. L and Ragland K. W., Combustion Engineering. McGraw-Hill, New York, 1998.

[17] Kays, W. M. and Crawford M. E., Convective Heat and Mass Transfer. 3rd ed., McGraw-Hill, New York, 1993.

[18] Westbrook, C. K and Dryer, F. L., Simplified Reaction Mechanisms for the Oxidation of Hydrocarbon Fuels in Flames, Combustion Science and Technology, 25, pp. 219-235, 1981.

#### NOMENCLATURE

$c_{p_m}$	Specific heat at constant pressure of the mixture
$c_{v_m}$	Specific heat at constant volume of the mixture
$D$	Mass diffusivity
$E_a$	Activation energy

$h_k$	Enthalpy of species $k$
$h_m$	Enthalpy of the mixture
$k$	Number of species
$k_{eff} = k_m + k_t$	Effective conductivity
$k_m$	Conductivity of the mixture
$k_t$	Turbulent conductivity
$k_G$	Global rate coefficient
$M_m$	Mixture molecular mass
$p$	Engine combustion chamber pressure in bar
$\dot{Q}_{rad}$ $\dot{Q}_{others}$	Volumetric generation/dissipation from radiation and other sources
$r_c$	Compression ratio
$R_k$	Volumetric generation rate from chemical reaction
$R_u$	Universal gas constant
$T$	Temperature in $K$
$u_j$	Fluid velocity
$X_j$	Coordinate in the three mutually perpendicular directions, $j = 1,2,3$
$T$	Time variable

#### GREEK SYMBOL

$\Delta H_c$	Heat of combustion
$\phi$	Fuel-air equivalence ratio
$\Phi_v$	Viscous dissipation function
$M$	Molecular viscosity

$\Omega$	Mass fraction
----------	---------------

### ДИНАМИКА САГОРЕВАЊА У ПОЛОЖАЈУ ГОРЊЕ МРТВЕ ТАЧКЕ КОД БЕНЗИНСКОГ МОТОРА

Л. Анетор, Е.Е. Осакуе, К. Одетунде

Модел бездимензионог бензинског мотора смо користили за систематско проучавање динамике сагоревања у положају г.м.т. код мотора – 5.734 л, V8. Модел укључује све експериментом уочене битне карактеристике у положају г.м.т. Нумерички модел је коришћен за испитивање динамике сагоревања при степену компресије  $r_c = 9,5; 10,5; 11,5$  и  $15,5$  и еквивалентном односу горива и ваздуха  $\phi = 1,0$ . Резултати показују да се за  $r_c = 15,5$  пуњење горива и оксидатора користи готово тренутно. Осим тога, подаци показују да је било потребно  $153,0; 52,6; 21,0$  и  $1,43\text{ms}$  при  $r_c = 9,5; 10,5; 11,5$  односно  $15,5$  да динамика сагоревања у цилиндру достигне вредност  $T^* = 1,0$ . За последњих  $0,01\text{ms}$ , код свих степена компресије, брзина промене притиска  $dp/dt$  је била у опсегу  $10^8 < dp/dt < 10^{14} \text{ Pa/s}$ , а одговарајућа температура  $2230 \leq T \leq 2700 \text{ K}$ . Истраживања такође показују да се са порастом степена компресије у горњој мртвој тачки монотонно повећава температура адијабатског пламена и топлота од сагоревања.